X-ray source system at the MSFC x-ray calibration facility

J. J. Kolodziejczak, R. A. Austin

Universities Space Research Association
ES-84, Marshall Space Flight Center
Huntsville, Alabama 35812

R.F. Elsner, M. K. Joy, M. Sulkanen

NASA
ES-84, Marshall Space Flight Center
Huntsville, Alabama 35812

E. M. Kellogg, B. J. Wargelin

Harvard-Smithsonian Center for Astrophysics
60 Garden Street, Cambridge, MA 02138

ABSTRACT

In preparation for calibrating the Advanced X-ray Astrophysics Facility, a multicomponent x-ray source system has been assembled for use at the x-ray calibration facility at MSFC. The system consists of an electron impact point source with filters, a penning gas discharge source, and two monochromators fed by rotating anode x-ray generator. The purpose and predicted performance characteristics of these elements are described as they apply to the AXAF calibration. The planned source characterizations, which will be performed in the June, 1995 through June, 1996 time period, are also described.

1. INTRODUCTION

The X-ray source system (XSS) described in this paper is being developed for use at the X-Ray Calibration Facility (XRCF) at Marshall Space Flight Center. It is a part of NASA's Advanced X-Ray Astrophysics Facility (AXAF) program. A key scientific goal for AXAF is to determine the observatory's x-ray response to a level near 1%. The XSS is an important component in the plan to implement this objective. A purpose of this paper is to describe the capabilities of the source system in terms of their relevance to AXAF calibration, therefore a brief description of the planned calibration process follows.

AXAF calibration is a three phase process. In their laboratories, instrument developers will perform the first phase by measuring the various characteristics of the flight instruments such as quantum efficiency, spatial resolution and energy resolution.[1,2] The metrology performed by Hughes-Danbury Optical Systems on the 4 parabolic and 4 hyperbolic shells, which combine to form AXAF's Wolter-I High-resolution mirror assembly (HRMA), is a phase-1 calibration on the x-ray optics as are the synchrotron measurements made at Brookhaven[3].

Once the various components are delivered, individual teams from the prime contractor, subcontractors, instrument development institutions, and MSFC will join forces for a 4-month-long 24-hour-per-day calibration marathon at the XRCF. A part of this time will be devoted exclusively to x-ray characterization of the HRMA using a set of instruments developed by personnel at the Smithsonian Astrophysical Observatory (SAO) called the HRMA X-ray Detection System (HXDS). The high count-rate capability of the HXDS relative to the flight instruments will permit a more precise HRMA calibration than would otherwise be possible, and will lead to a more balanced understanding of the telescope response relative to the instrument response. The instrument response will already be well understood as a result of phase-1 calibration. The remainder of the time will be devoted to HRMA plus flight instrument calibration which includes the only ground x-ray calibration of the assembled flight gratings. Some of this grating work will also use the HXDS capabilities.

0-8194-1874-9/95/$6.00

The third phase of calibration will happen on-orbit where a number of reasonably well-understood and stable astrophysical x-ray sources will be observed. These data will continue to accrue throughout the life of AXAF to maintain adequate understanding of those observatory characteristics which may change over time.

2. CALIBRATION AT THE XRCF

At a distance of 528 m, a 0.5 mm object subtends 0.2 arcsec. These respective dimensions are the source-to-HRMA distance, nominal source size, and expected FWHM of the HRMA point-response function. Figure 1 shows the XRCF. At one end, Building 4718 houses the 22.9-m-long-by-7.3-m-diameter instrument chamber and associated control rooms. At the other end, building 600 houses the XSS. 38m from the XSS is building 500 which houses a portion of the beam monitoring equipment.

During AXAF X-ray calibration a variety of x-ray source configurations will be used to illuminate the HRMA. Detectors near the HRMA and in building 500 will continuously monitor the output. A flow proportional counter (FPC) mounted on a moving stage and a solid state spectroscopic detector (SSD) will monitor the flux in building 500, while an array of 4 flow proportional counters surrounds the HRMA entrance aperture. One of these is also on a remotely controlled stage.

These detectors will also be used for on-axis characterization of the XSS. Off-axis tests will use a High Resolution microchannel-plate Imager (HRI)[4]. The specific planned characterizations are described in later sections.

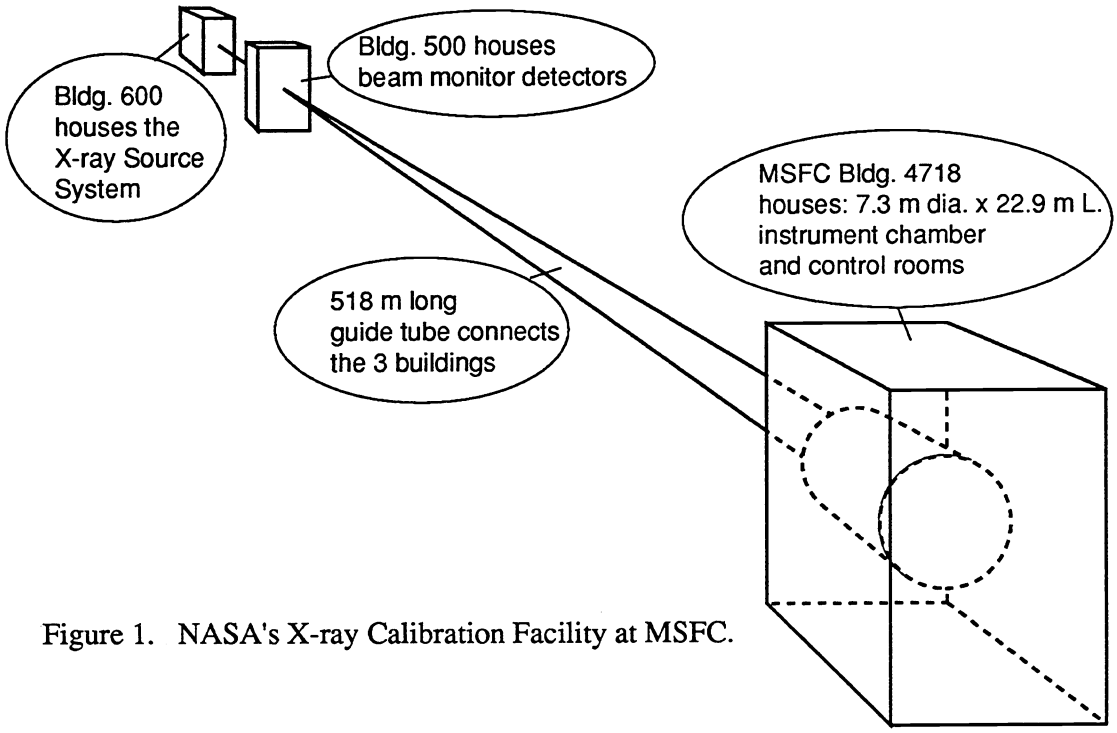

Figure 1. NASA's X-ray Calibration Facility at MSFC.

3. CAPABILITIES THE XSS NEEDS TO PROVIDE

The design of the XSS was driven by the performance capabilities of AXAF, in terms of spatial and energy resolution, efficiency and count rate limits. The result was a collection of x-ray generators, filters and

monochromators which satisfy specific needs as well as more general requirements. The sensitivity of AXAF model parameters to energy, spectral purity and source size was also considered in selecting suitable source configurations.

3.1 Source Size

The half power diameter of the HRMA point response function is expected be <1 arcsec over much of its energy range so a 0.5 mm maximum source size is chosen to minimize source contributions to the image while still permitting a reasonable flux without damaging a target. The image of the 0.2 arcsec source would contribute <8% to the measured 1 arcsec encircle energy. High resolution pinhole images of the sources using the HRI during characterization will provide the data necessary to account for the finite source size to the necessary accuracy[4].

3.2 Spectral Purity

The lack of energy resolution in the two microchannel plate detectors requires a beam which is free of both lines at widely differing energies and as much continuum as possible. Both the high-resolution camera (HRC) flight instrument, and high-speed imager(HSI) HXDS instrument will provide data which is more directly related to models if high spectral purity is maintained. We will use an electron impact source with continuum removing filters to provide clean lines. At interesting energies where such lines do not exist, monochromators may be needed.

3.3 Intensity

Both the counting rate limits and the surface brightness limits of the detectors define the source intensity range. Table 1 lists approximate values for these parameters:

Instrument	count rate limit sec^{-1}	brightness limit $cm^{-2}\ sec^{-1}$
HRC	200	2×10^5
ACIS	200	10^3
HXDS-SSD	20000	10^{11}
HXDS-FPC	20000	10^{11}
HXDS-HSI	2000	5×10^6

Table 1. Approximate count rate and detected brightness limits for the various instruments to be used at the XRCF.

The FPC and SSD numbers are derived from the smallest apertures available on those detectors (5 micron diameter). A large dynamic range in source intensity is clearly desirable to take full advantage of this assortment of detectors. The brightness limit for the AXAF CCD Imaging Spectrometer (ACIS) is based on a limit of 1 photon per 32-64 pixels per frame. The ACIS value accounts for a factor of 0.1 to limit the Poisson probability of getting 2 or more photons per frame to 1% for in-focus on-axis measurements where most of the counts are contained within a few pixels. As an example, from these numbers we can derive a maximum acceptable source intensity as low as 3×10^6 photons $sr^{-1}\ sec^{-1}$ for ACIS point spread function measurements and as high as 10^{12} photons $sr^{-1}\ sec^{-1}$ for core measurements with the SSD and 5 micron pinhole. Both of these cases are for 1.5 keV photons.

3.4 Line widths

Measurements need to be made of the resolution and line spread functions of the low energy transmission grating (LETG) and high energy transmission grating (HETG). The later consists of medium energy gratings (MEG) and high energy gratings(HEG). All three of these should have resolving power greater than 1000 near

the low-energy ends of their spectral ranges and therefore require narrow lines for calibration. The low-energy end of the HEG is 1 keV and the Mg-K line at 1.25 keV is naturally narrow with E/dE>3000. The energy range of the LETG extends to below 0.1 keV and the 0.095 eV Al-IV & V line produced by a continuous discharge Penning source[5] with E/dE>10000 should be acceptable. The energy range of the MEG extends down to ~0.2 keV. For this the 0.277 keV C-K line narrowed to E/dE>2000 using a grating monochromator is planned, however, recent work on the Penning source[6] has shown that a bright Ar-I line at 0.22 eV is attainable and may be narrow enough. Preliminary measurements indicate E/dE>1000 for this line.

3.5 Photon energies

A part of the phase-1 calibration of AXAF components includes synchrotron measurements to map details in the spectral response[3,7,8]. Time constraints prevent complete duplication of this effort at the XRCF, however spot checks in critical energy ranges and coarse spectral scans to search for unexpected features are needed for validation of combined models. A grating monochromator for low energies and a crystal monochromator for high energies, both supplied by high-output sources, were selected to fulfill this need. E/dE in the range 30-100 is sufficient for these measurements.

3.6 Other

Constraints on beam spatial uniformity, source mechanical stability, power supply electrical stability, change out time, and other elements of the system have arisen from the 1% AXAF calibration goal as well as test time constraints.

4. X-RAY SOURCE SYSTEM

Figure 2 shows a block diagram of the x-ray source system. All the components are mounted on four carts which ride on rails. The rails are attached to a 3 m x 3 m optical table. The table is mounted on a vibration isolated concrete pier. A stationary filter chamber mates with the end of the guide tube and provides a common interface for the equipment on each of the 4 carts. One cart supports the electron impact point source. Another supports the grating monochromator (HIREFS®) and rotating anode source. A third supports the crystal monochromator (DCM) and a second rotating anode source. Finally, the fourth supports either the Penning source or an unencumbered rotating anode source. Each of these components is discussed below.

4.1 Penning Source

In the penning source[5], gas discharge current ionizes gas atoms which then impact cathode targets and sputter ionized metal atoms into the gas. Further collisions generate numerous bright EUV and soft x-ray lines. We currently plan to use Argon gas and Al cathodes to produce the needed Al-IV and Ar-I lines for LETG and MEG calibration, however we will also investigate alternative gases like P10 to try to excite the C-K line. The water-cooled Penning source heads for the XSS were built by Smithsonian Astrophysical Observatory.

Gas pressure is set to ~25 mTorr to start the Penning source, then a current limit is set ~500 mA and voltage is adjusted until ignition. Pressure is reduced as low as possible to maximize flux and either current or voltage are set to adjust the flux up to the maximum current. The current limits the system since the source does not run at maximum voltage when the current is maximum. Table 2 summarizes the performance characteristics:

Maximum current	1000 mA
Source size	0.5 mm wide slit in the LETG dispersive direction
Expected flux	$>10^{10}$ sr^{-1} sec^{-1} per line
E/dE	>15000 @ 0.095 keV[9]; >1000 @ 0.22 keV[6]
Cathode lifetime	4 hr
Target material	Aluminum
Gas	Argon

Table 2. Penning source performance characteristics.

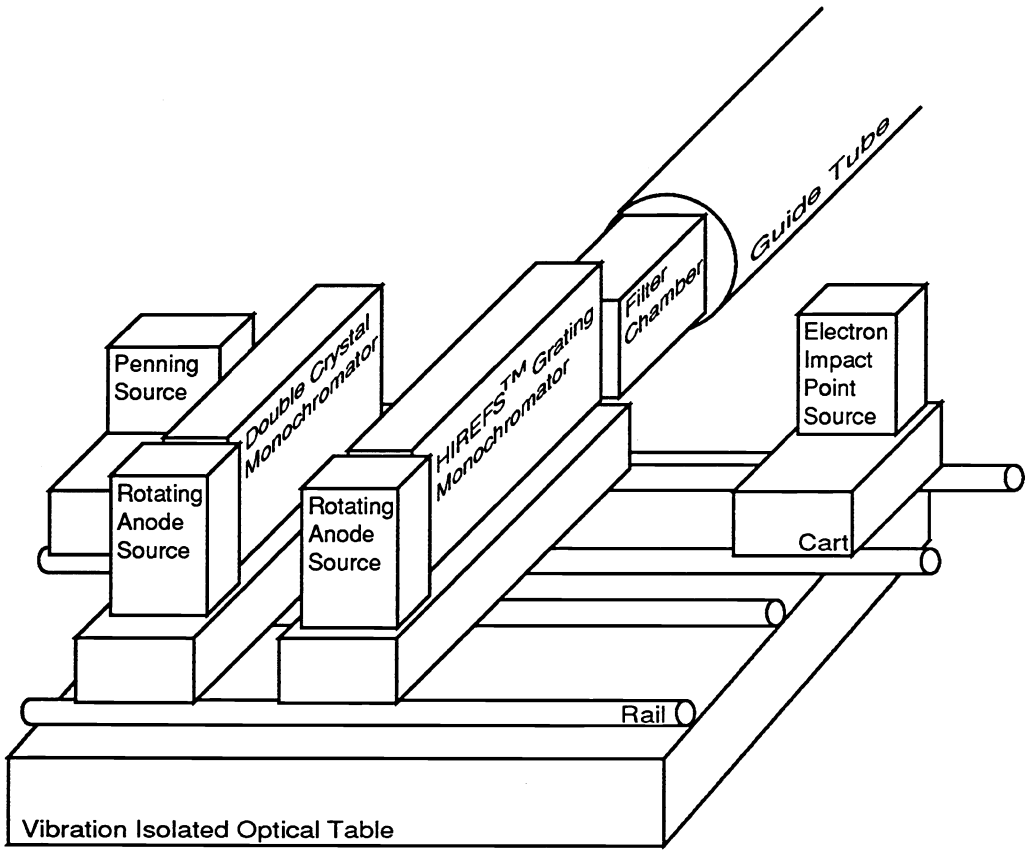

Figure 2. The XRCF X-ray Source System

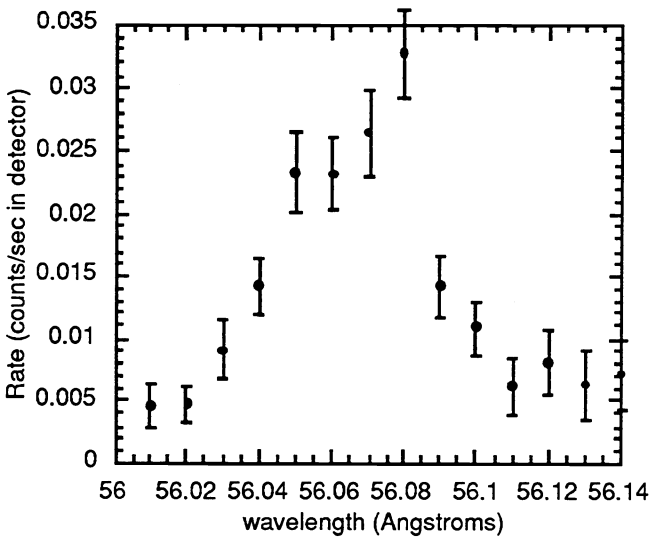

Figure 3. Spectrum from the penning source using HIREFS® monochromator with 10 μm entrance slit and 5 μm exit slit with channeltron detector, 1 kV, 600 mA, 6 mTorr, Argon gas, Aluminum cathodes. The theoretical HIREFS® resolution is 0.028 Angstroms, and the measured FWHM is 0.04 Angstroms, so the resulting FWHM of the line is 0.028, which gives an E/dE of 2000.

Before using the Penning source for AXAF calibration, we will need to determine the following: 1) dependence of output flux upon current, and gas pressure in the manifold, 2) variation of source flux over time (temporal stability), and 3) characterize the Ar I, 0.22 keV and the Al IV, 0.095 keV lines. The emission region of the Penning source has a diameter of a few millimeters, so the source will be operated with a slit aperture which will define the source size, and pinhole camera images of the source will be unnecessary. Measurements 1 and 2 will be performed in the on-axis configuration with the Bldg. 500 FPC serving as the detector. These important measurements will answer practical questions such as: what current and pressure settings give optimum performance and how long for a particular current and pressure can we operate the source before change-out is necessary. Spectral characterization will be made off-axis with the HIREFS® configured as a spectrometer and the HRI serving as the detector. Resolving powers of > 2000 will be adequate for measuring the positions, widths (at least upper limit determinations), and relative intensities of the 0.22 keV and 0.095 keV calibration lines and nearby lines which might complicate calibration of the LETG and HETG spectrometers. Preliminary measurements with HIREFS® in a monochromator configuration and a Channeltron detector[6] suggest these two lines will adequately serve our calibration needs. Figure 3 is a plot of the Penning source data from this preliminary experiment.

4.2 Electron Impact Point Source and Filters

The electron impact point source is a modification of the one used for the VETA-I test[4]. The modifications include a new bias cup design with independent bias control and a new power supply. The anodes or targets are oil-cooled and quickly replaceable so that a variety of materials can be selected to generate the required lines. The filter wheel assembly houses two independently controllable filter wheels which will include open positions for unfiltered output. The filter wheel assembly is a stationary element so each source subsystem interfaces to it and the x-ray beam always passes through it. Table 3 summarizes the performance characteristics of these items.

Voltage Range	1-30 keV
Current Range	0.050-5.0 mA (70 W max.)
Source size	0.5 mm x 0.5 mm
Take-off angle	30°
Expected count rates	see figs. 4 and 5
Target materials	see table 4
Filter Wheels	2
Filter positions per wheel	32
Filter Materials	2,4, and 6 mfp selectable, see table 4

Table 3. Electron impact point source performance characteristics.

Filters are selected for each target in 2 and 4 mean-free-path thicknesses and since there are two wheels, 2, 4, or 6 mean free path filter choices are currently planned. The list of targets and filters includes those in table 4. The final two columns in this table list the voltage and filter thickness combination which optimizes the line-to-continuum ratio. Figures 4 and 5 show the predicted HRC and ACIS count rates per mA for most of these targets. Where the modeled materials differ from the currently planned materials, the modeled materials appear in parentheses in table 4.

The predictions given in Figures 4 and 5 are base on a physical radiation transport model[10] and are convolved with current HRMA and instrument models which are shown in ref. 11. Accuracy of a factor of 2-3 is assumed. The fluxes are expected to be adjustable, up a factor of 5 and down a factor of 20, using the current adjustment. Figure 5 shows that the intensity range does not extend low enough for in-focus measurements with ACIS for any of the lines above 1 keV, since we will need count rates below 1 sec^{-1} and the values in this range are almost all more than 50 sec^{-1}. Two options for dealing with this problem may be considered: (1) thicker filters, or (2) lower voltage. Although thicker filters would continue to improve the line-to-continuum ratio for most cases, there is a problem in that a small percentage variation in the thickness can lead to substantial beam nonuniformity. The preferred option would be to lower the voltage, for example, the

worst case is Cr with over 600 counts sec^{-1} mA^{-1} at 5 times the line energy and 6 mfp, but at 2 times the line energy and 6 mfp (case not shown) the rate is only 70. At 1.2-1.3 times the line energy an acceptable intensity is likely. This lowering of the operating voltage will be at the expense of line-to-total-continuum ratio, but the energy resolution of ACIS will probably still permit a good measurement of counts in the line using spectral fitting algorithms[12].

A similar problem exists with the HRC but to a smaller extent and lowering the voltage is still likely to be the preferred option. For the same example, the simulation indicates that reducing the voltage on the Cr target from 5 to 2 times the line energy reduces the rate from 118 to 13 sec^{-1} mA^{-1} while the line fraction only changes from 0.85 to 0.75. Obviously, the uncertainties in the simulation will require us to measure the source intensity and repeat this analysis to assure that acceptable counting rates can be achieved.

Material	Energy (keV)	Filter	mfp (μm)	Best V (x line energy)	Best t (x mfp)
Al	1.486	Al	9.19	3	6
B	0.183	B	1.27	4	6
Be	0.1085	Be	0.903	4	6
C	0.277	C_8H_8	5.16	4	6
Cr	5.41	V	22	5	6
Cu	8.03	Ni	24.1	5	6
Fe	6.4	Mn	22.6	5	6
Mg	1.254	Mg	11.8	3	6
N from TiN	0.3924	Ti	0.5	3	4
Ni	7.47	Co	23.2	5	6
O from SiO_2	0.5249	Cr	0.432	3	6
Ti	4.51	Ti	20.3	5	2
Zn	8.62	Cu	27.3	3	6
Ag	2.98	Rh (Ag)	2.5 (1.87)	5	2
Au	9.71	Ta (Au)	6.2 (6.4)	3	6
Co	0.7762	Co	0.58	3	6
Cu	0.9297	Cu	0.72	3	6
Cr	0.5728	Cr	0.51	3	6
Fe	0.705	Fe	0.59	3	6
Mo	2.293	Nb (Mo)	2.5 (1.62)	2	6
Ni	0.852	Ni	0.624	3	6
Sn	3.444	Cd (Sn)	2.5 (3.17)	5	2
Ti	0.4522	Ti	0.663	3	6
W	8.398	Cu	25.2	3	6
Zn	1.012	Zn	0.94	5	6
Zr	2.04	Zr	1.98	2	6

Table 4. Point Source Targets and Filters. Best V and best t are the combination of voltage (in the range from 2 to 5 times the line energy) and thickness (in the range from 0 to 6 mfp) that gives the highest simulated line-to-total-continuum ratio.

Driven by the scientific requirements for AXAF calibration, we have determined that the following parameters must be verified to fall within certain limits or be characterized to sufficient accuracy: source size, source concentration, temporal stability, positional stability, operating range, output flux. To verify that the source diameter is no greater than the required 0.5 mm, pinhole camera images will be taken of the source,

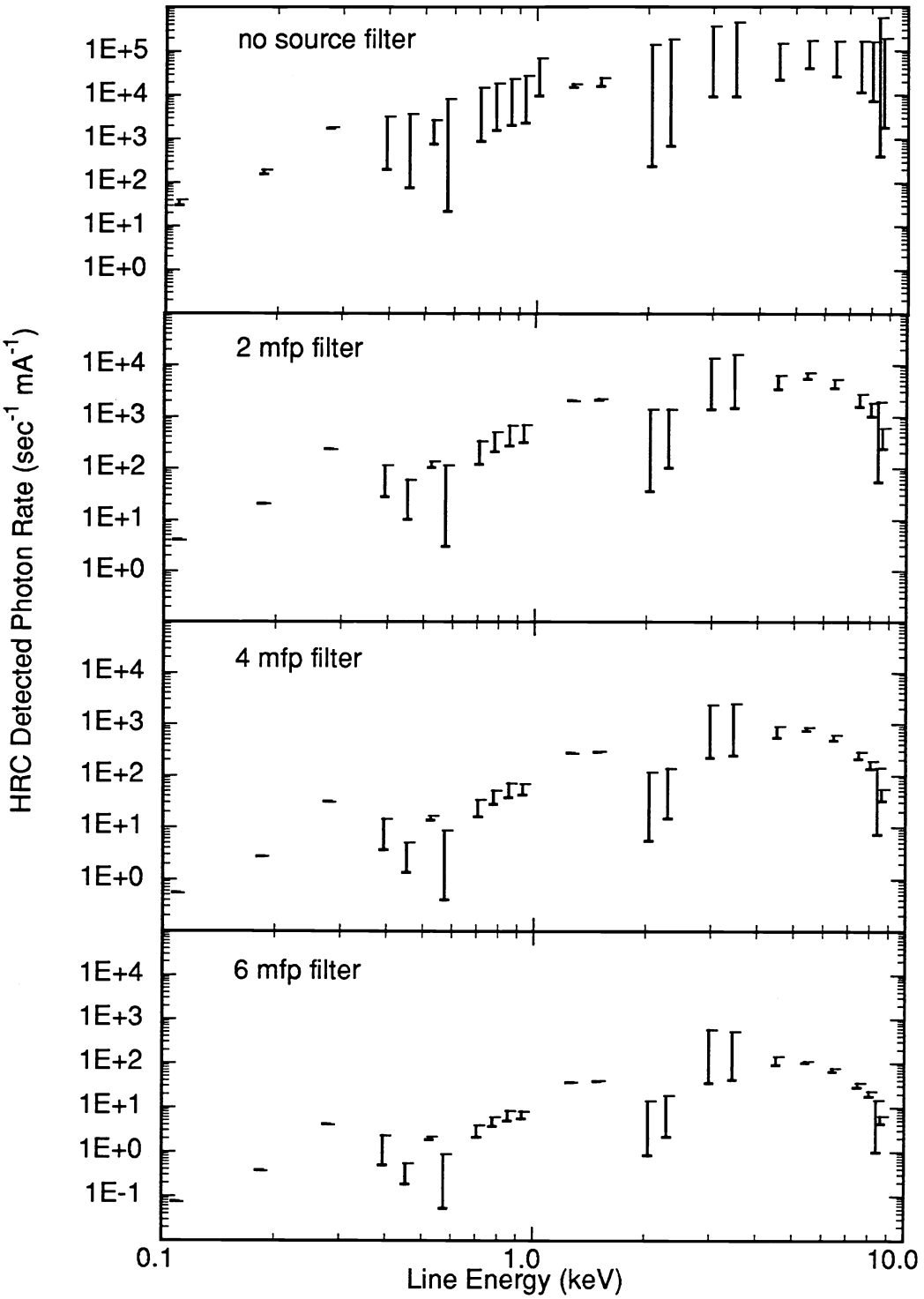

Figure 4. Predicted CsI-coated HRC detected photon rates at voltages from table 4. The top of each bar is the total rate and the bottom is the rate in lines.

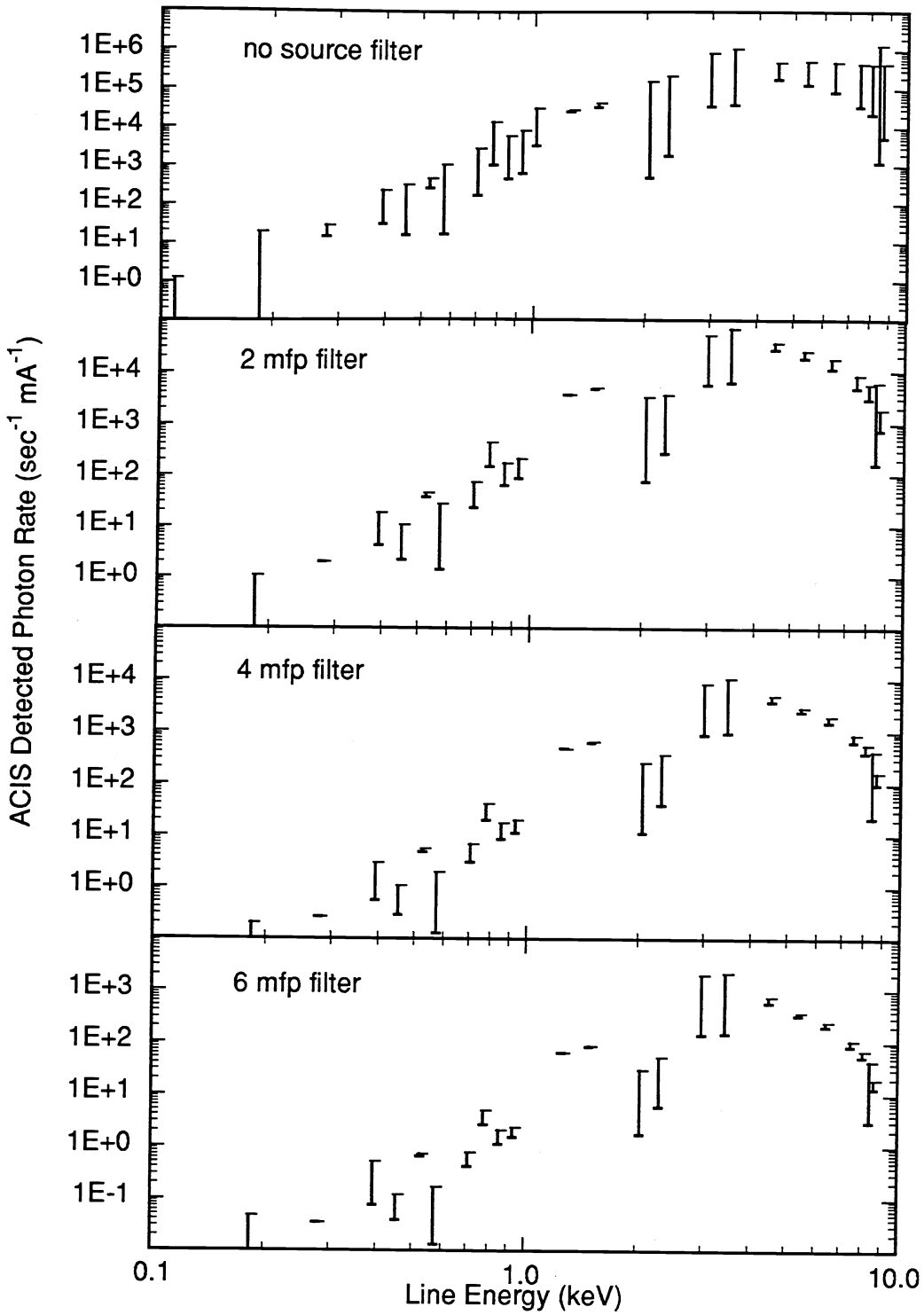

Figure 5. Predicted front-side-illuminated ACIS detected photon rates at voltages fromTable 4. The top of each bar is the total rate and the bottom is the rate in lines.

off-axis, for each of the 25 or so anode materials over a range of bias voltages and anode voltages and currents. Pinhole sizes (diameters 25(m and 70(m) and source-pinhole, pinhole-HRI distances will be chosen to assure that better than the budgeted 0.1 mm image resolution is maintained. Pinhole images will also provide information about source concentration (i.e., verify that intensity from the source falls below 10-4 of its peak value at distances greater that 0.25 mm from the center of the spot), and the range of voltages and currents over which a compact source can be maintained. Output flux will be measured on-axis with the BND-500 FPC and SSD. For a given anode, these measurements will allow us to choose the necessary anode voltage and current settings to obtained a desired output flux. Temporal stability will be characterized during beam mapper scans which will be made to determine x-ray filter uniformity (see below).

To adequately characterize the x-ray filters, measurements of absolute transmission, scattering and vignetting will need to be made. For each anode/filter combination, absolute transmission will be measured to an accuracy of 5% or better. To ensure that no filters having pinholes will be used for the calibration, the FPC beam mapper will make measurements at 36 points over the region of the filter which intercepts the beam reaching the HRMA. Filters having greater-than-normal nonuniformity will be discarded. By mapping the beam, we will also be able to determine if beam is being vignetted by the filter wheel assembly. To determine if the filter wheel assembly is producing any scattering of the beam, an occulting disk mounted on the Bldg. 500 beam mapper will be placed in the beam. If there is no scattering, no x-rays will be detected by the detectors at the HRMA entrance.

4.3 High-Output Source

To obtain a usable count rate through the monochromators, and especially in the case of the high resolution line at C (0.277 keV), a more powerful source than the point source described in section 4.2 is necessary. To satisfy this need we selected a rotating anode x-ray generator system manufactured by Rigaku Corp. In this water-cooled system, the anode is a beveled disk rotating at 6000 rpm. By selecting a low take-off angle, a line shaped electron beam can be projected into a point-like x-ray source. Figure 6 illustrates this. Table 5 is a summary of the rotating anode source performance characteristics.

anode materials	W or C
anode take-off angles	14° for HIREFS® 7° for DCM and unencumbered
cathode sizes	C1: 0.2mm x 2 mm/ 5-25 kV C2: 0.2mm x 2 mm/ 20-40 kV C3: 0.5mm x 10mm/ 5-25 kV
Voltage range	5-40 kV in 1 kV steps
Current Range	10-450 mA in 3 mA steps
Power	C1 or C2 with W: 2500 Watts C1 or C2 with Carbon: 300 Watts C3 with Carbon: 2000 Watts C3 with W: 15000 Watts
Intensity	~>10^{14} sec^{-1} sr^{-1} in C-K line see fig. 7 for W
Source sizes	for HIREFS®: C3: 0.5 mm wide x 2.5 mm high C1/C2: 0.5 mm wide x 0.2 mm high for DCM and unencumbered: C1/C2: 0.25 mm wide x 0.2 mm high C3: 0.5 wide x 1.2 mm high

Table 5. Rotating anode source performance characteristics.

Figure 7 shows the predicted source flux from the W anode. The low-energy intensity decreases with increased voltage, in part, because of the low take-off angle which requires a longer path for a generated photon to escape from the material and therefore more absorption for the more deeply penetating high voltage

electron. As a result, we will always want to run the rotating anode source at the lowest possible voltage when using the grating monochromator. We will need to tune the voltage to the appropriate value for a given energy when using the crystal monochromator.

The RAS, being much like the EIPS, will be characterized in the same way. In this case there will be only two anode materials, W and C.

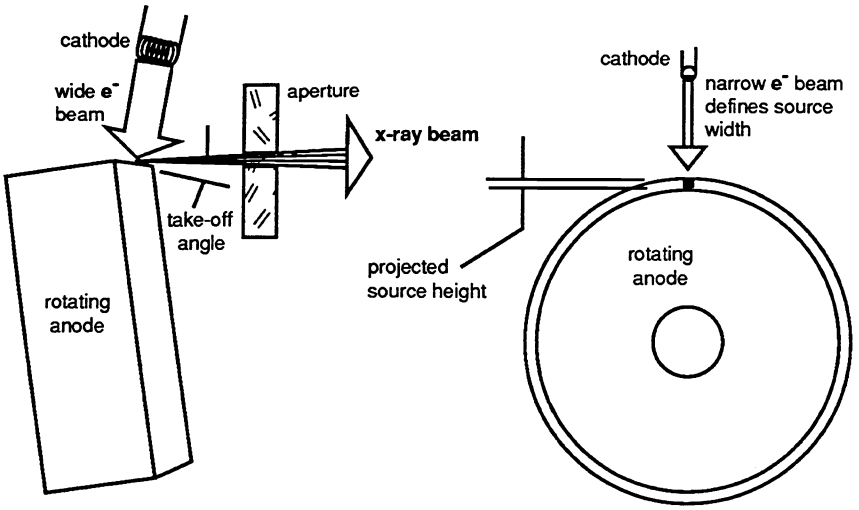

Figure 6. Diagram of the rotating anode source.

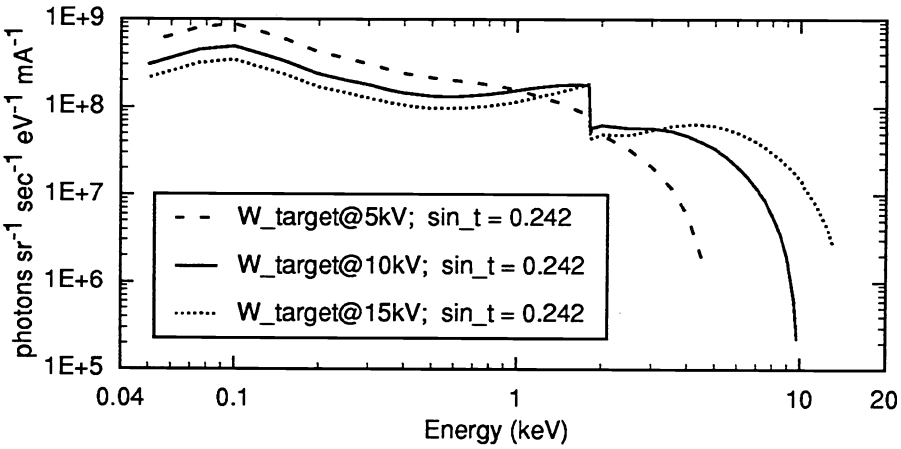

Figure 7. Source Intensity for Tungsten at 3 energies ant 14° take-off angle.

4.4 Grating Monochromator

A HIREFS®–SXR-1.75 grating monochromator[13] from Hettrick Scientific Inc. (HSI) was selected for low energy applications below ~1.5 keV since it has fixed entrance and exit slit locations and a sufficient range of resolution settings to satisfy both our need for narrow lines to examine the grating line response, and the requirement to perform low resolution efficiency scans. HIREFS® stands for High Resolution Erect Field Spectrometer. The addition of an exit slit converts it to a monochromator.

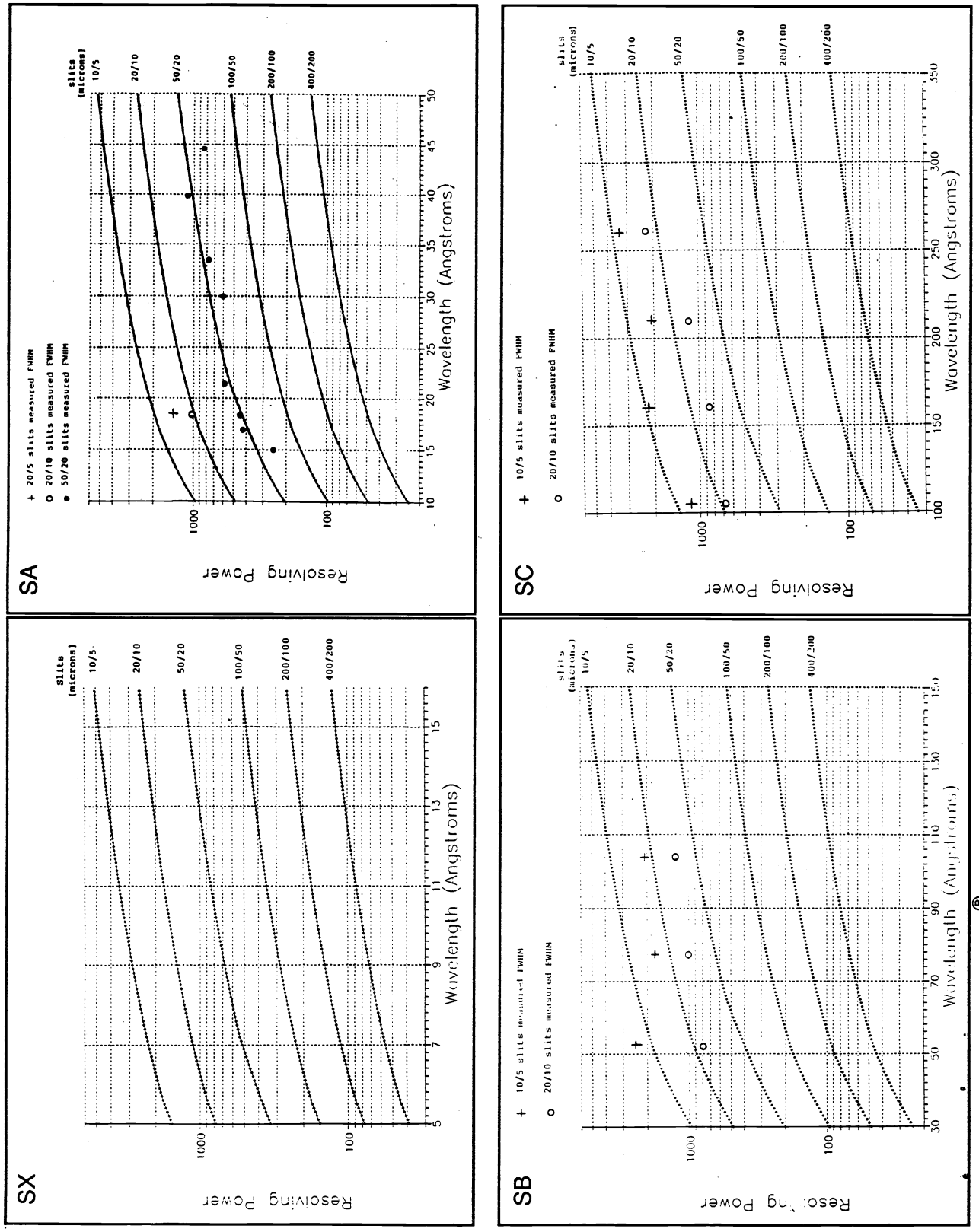

Figure 8. HIREFS® grating monochromator energy resolution vs. wavelength. Curves and data are from ref. 13.

The path of photons through the HIREFS® begins as they pass through an adjustable entrance slit and reflect off a gold-coated cylindrical mirror which focuses the beam in the non-dispersive direction. This mirror is adjustable to permit beam focusing directly onto the exit slit for high spatial resolution or up to 1.9 m outside the exit slit to provide a factor of ~3 increase in throughput. A second gold-coated mirror, this one spherical, focuses the beam in the dispersive direction over the distance to the exit slit. Along the way the beam is intercepted by a reflection grating which disperses only the selected wavelength to the adjustable-width exit slit. The beam is always focused by the spherical mirror in the dispersive direction at the exit slit, however the output of the slit would be astigmatic were it not for the initial cylindrical mirror which corrects for the astigmatism if adjusted to focus on the exit slit.

Number of selectable gratings	4 (SX,SA,SB,SC)
Energy Range	SA: 0.77-1.6 keV SB: 0.25-0.83 keV SC: 0.08-0.28 keV SX: 0.04-0.12 keV
Energy resolution	See Fig. 8
Output beam intensity	See Fig. 9
Entrance slits	small slits: 5, 10, 20, 50, 100, 200 μm medium slits: 75,100,150,200,300,400 μm
Exit slits	5, 10, 20, 50, 100, 200 μm

Table 6. Performance characteristics of the HIREFS® monochromator.

Energy resolution is adjustable by changing the entrance and exit slit widths. The resulting resolving power depends on wavelength as shown in Figure 8. The points plotted in Figure 8 are measured values of the energy resolution performed by HSI using a laser plasma source prior to delivery of the monochromator.

The beam intensity will naturally be a function of both wavelength and resolving power. Figure 9 is plots the predicted output intensity based on a simple scalar diffraction grating model which includes reflections from the 2 mirrors and the grating. Plots of the first 3 order are shown, and indicate that higher orders may be a significant contributor to the output up to about 0.8 keV. We intend to investigate the use of filters to reduce higher orders, but their effects must be considered when planning AXAF calibration measurements.

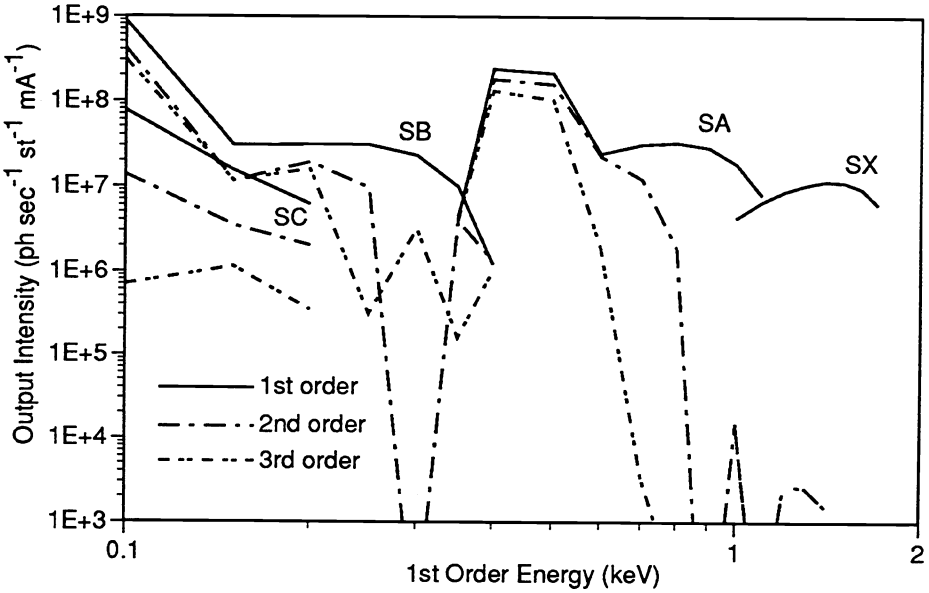

Figure 9. Predicted intensity out of HIREFS® monochromator with 200/100 μm entrance/exit slits.

The two monochromators will pose the most formidable characterization challenge. The following must be determined: 1) absolute energy scale in the range 0.1-2 keV, 2) energy resolution, 3) throughput, 4) source size, 5) beam angular size, 6) intensity uniformity, 7) temporal stability, 8) spectral purity, and 9) higher order diffraction. Measurements of 1 and 2 will be performed off-line by scanning through narrow lines provided by the Penning and electron impact point sources; the HRI will serve as the detector. By using lines with well known energies, we can pin down the energy scale of the HIREFS®. By making wavelength scans of intrinsically narrow lines it will be possible to determine the energy resolution of the HIREFS® or at least determine if the energy resolution is adequate at a particular energy. Pinhole camera measurements made off-axis will be used to measure the source size in the non-dispersion direction. The remaining measurements, 3, 5, 6, 7, 8, and 9 will be made on-axis with the Bldg. 500 FPC and SSD. With the rotating anode source connected to the HIREFS®, throughput measurements will be made for a variety wavelength settings and source voltage/current settings. For this same configuration, beam angular size, intensity uniformity, and temporal stability will characterized during beam maps over the region of the beam which will intercept the HRMA. The degree of spectral purity and higher order diffraction will be determined by examining energy spectra obtained with the FPC and SSD.

4.5 Crystal Monochromator

The crystal monochromator for the XSS was designed and built by the National Institute of Standards and Technology (NIST)[14]. This double crystal design has two 5-position turrets which hold the various crystals. Photons enter through an entrance slit, and those with the selected energy are reflected at the Bragg angle off the two crystals into a parallel, but offset, beam. The Crystals selected are Silicon , Germanium, Potassium Dihydrogen Phosphate (KDP), and Thallium Acid Phthalate (TAP).

Number of selectable crystal	5 positions available, 4 used (Si, Ge, KDP,TAP)
Minimum/Maximum Bragg Angle	19.88°/81.60°
Energy Range	Si-400: 4.62-13.42 keV (2d=2.71551 Ang.) Ge-111: 1.92-5.58 eV (2d=6.53287 Ang.) KDP-011: 1.23-3.572 keV (2d=10.20773 Ang.) TAP-001: 0.49-1.41 keV (2d=25.7568 Ang.)
Energy resolution	See Fig. 10
Output beam intensity	See Comments in Text
Entrance slits	0.3 mm
Exit slits	None

Table 7. Performance characteristics of the double crystal monochromator.

Figure 10 shows the energy resolution of the various crystals. For the purposes of estimating count rates for AXAF calibration planning we will assume the throughput to be 1% (nominally 10% efficiency from each crystal) of the flux from the W-anode rotating anode source as shown in figure 7. To minimize contributions from higher orders in the DCM we may need to detune the angles of the crystals, and the effect of this detuning on the count rate has not yet been predicted.

Characterization of the DCM will following nearly an identical procedure as above and the following must be determined: 1) absolute energy scale in the range 1-10 keV, 2) energy resolution, 3) throughput, 4) source size, 5) beam angular size, 6) intensity uniformity, 7) temporal stability, 8) spectral purity, and 9) higher order diffraction.

5. SYSTEM OPERATION

During AXAF calibration, a test conductor has the job of managing the overall test procedure. Requests from the test conductor for changes to the source configuration will come via a computerized procedure script. Since the 4 month measurement time will be tightly scheduled, the XSS has been designed to make every type of change as quickly as possible. The 4 carts which support the different configurations slide across the rails into position and are then lowered onto a set of precision hard points. These hard points are precisely

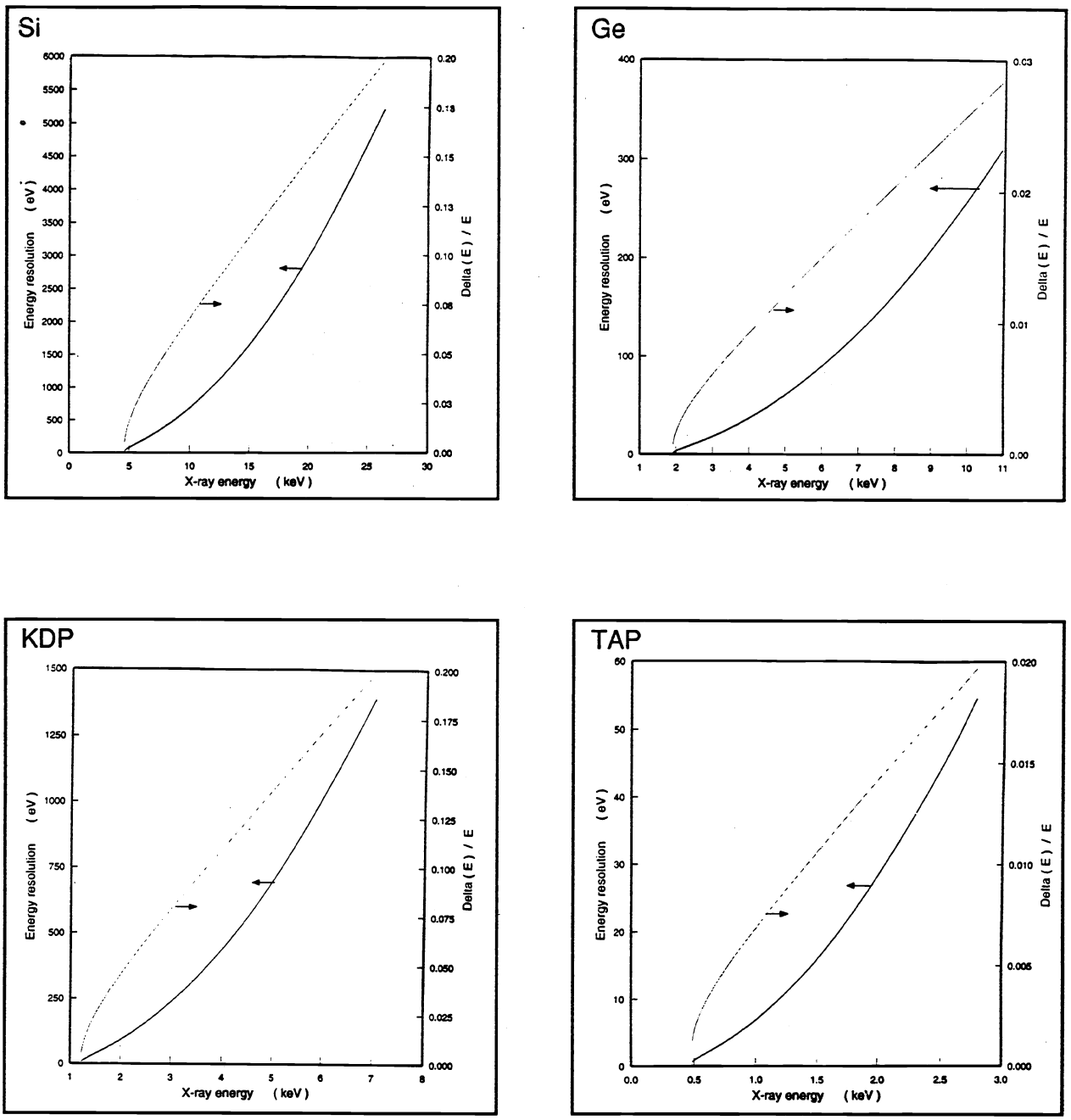

Figure 10. NIST Double crystal monochromator energy resolution vs. energy. Curves are from ref. 14.

sized pins attached to thick steel pillars which are in turn, rigidly mounted to the optical table. They are used to insure repeatable repositioning of each source without extensive realignment after each configuration change.

Data describing which configuration is active, and its electrical and mechanical parameters will be stored each time something changes and at frequent regular intervals throughout the test. Whenever possible, critical parameters like voltage, current, and wavelength settings will be automatically entered. Other parameters, like which anode is being used, and alignment parameters, will be prompted by computer and manually entered.

6. REFERENCES

1. D. Dewey, D.N. Humphries, G.Y. McLean, D.A. Moshella, "Laboratory Calibration of X-Ray Transmission Diffraction Gratings", *Proc. SPIE*, Vol. 2280, pp. 257-271, 1994.

2. K.A. Flanagan, M. Barbera, S. Murray, M. Zombeck, "Calibration program for the AXAF High Resolution Camera", *Proc. SPIE*, Vol. 2280, pp. 243-256, 1994.

3. D.E. Graessle, R.J. Brissenden, J. Cobuzzi, J.P. Hughes, E.M. Kellogg, F.E. Mootz, D.A. Schwartz, P.O. Slane, M.V. Zombeck, R.L. Blake, J. Davis, "Feasibility study of the use of synchrotron radiation in the calibration of AXAF: initial reflectivity results", *Proc. SPIE*, Vol. 1546, pp. 13-25, 1991.

4. P. Zhao, E.M. Kellogg, D.A. Schwartz, Y. Shao, M.A. Fulton, "Intensity Distribution of the X-ray Source for the AXAF VETA-I Mirror Test", *Proc. SPIE*, Vol. 1742, pp. 26-39, 1992.

5. D.S. Finley, S. Bowyer, F. Paresce, and Roger F. Malina, "Continuous discharge Penning source with emission lines between 50A and 300A", *Applied Optics*, Vol. 18, No. 5, pp. 649-654, 1992.

6. E.M. Kellogg, B.J. Wargelin, T.J. Norton, J.J. Kolodziejczak, "Penning Source for calibration of x-ray and EUV optics and spectrometers at wavelengths as short as 50A", *Proc. SPIE*, this volume, 1995.

7. C.S. Nelson, T.H. Markert, Y.S. Song, M.L.Schattenburg, D.E. Graessle, K.A. Flanagan, R.L. Blake, J. Bauer, E.M. Gullikson, "Efficiency measurements and modeling of AXAF high energy transmission gratings", *Proc. SPIE*, Vol. 2280, pp. 191-203, 1994.

8. M. Barbera, D. Breslau, K. Flanagan, D. Graessle, M. Zombeck, "Synchrotron x-ray transmission measurements in the calibration program for the UV/Ion Shields of the AXAF HRC", *Proc. SPIE*, Vol. 2280, pp. 229-242, 1994.

9. M. C. Hettrick, J.H. Underwood, P.J. Batson, M.J. Eckart, "Resolving Power of 35000 (5 mA) in the extreme ultraviolet employing a grazing incidence spectrometer", *Applied Optics*, Vol. 27, No. 2, pp. 200-202, 1988.

10. M.E. Sulkanen, J.J. Kolodziejczak, G. Chartas, "Numerical simulation of electron impact x-ray sources", *Proc. SPIE*, this volume, 1995.

11. M.C. Weisskopf, S.L. O'Dell, R.F. Elsner, L.P. VanSpeybroeck, "AXAF-- an overview", *Proc. SPIE*, this volume, 1995.

12. G. Chartas, K.A. Flanagan, J.P. Hughes, E.M. Kellogg, D. Nguyen, M.V. Zombeck, M. Joy, J.J. Kolodziejczak, "Correcting x-ray spectra obtained from the AXAF VETA-I mirror calibration for pile-up, continuum, background and deadtime," *Proc. SPIE*, Vol. 1742, pp. 65-74, 1992.

13. M. C. Hettrick, Instruction Manual for the HIREFS®-SXR-1.75 Base Monochromator, July, 1993.

14. J.-L. Staudenmann, R.D. Deslattes, Design Principles of the AXAF-I monochromator, July, 1994.